Astron. Astrophys. 353, 655–665 (2000)

ASTRONOMY AND ASTROPHYSICS

Chemical abundances from Magellanic cloud B stars⋆

A.J. Korn[1,2], **S.R. Becker**[1], **C.A. Gummersbach**[2], **and B. Wolf**[2]

[1] Universitäts-Sternwarte München (USM), Scheinerstrasse 1, 81679 München, Germany
[2] Landessternwarte, Königstuhl, 69117 Heidelberg, Germany

Received 9 August 1999 / Accepted 8 November 1999

Abstract. In recent years, B stars have been established as reliable tracers of present day abundance patterns. They yield an independent set of abundances from He to Fe which can be cross-checked against other sources such as H II regions and cool supergiants. In this paper, we present purely spectroscopic analyses of 9 non-supergiant B stars ($13 < \mathrm{m}_V < 15$), 5 of which located in the young populous clusters NGC 1818, 2004 (LMC) and NGC 330 (SMC), the other 4 being MC field stars. CASPEC spectra (4000 Å $< \lambda <$ 5000 Å) with R $\sim$ 20 000 and S/N $\sim$ 100 are used to determine $T_{\rm eff}$, $\log g$, ξ and the abundances of oxygen and silicon *simultaneously*. Particular attention is paid to a consistent treatment of the metallicity of the underlying atmosphere. Kurucz ATLAS 9 LTE atmospheres and DETAIL/SURFACE non-LTE line formation (H, He, C, N, O, Mg, Al, Si and Fe) are used throughout the analysis.

While we find little difference between the abundances from cluster members and field stars, the behaviour of N is surprising: it is generally enriched with respect to the H II value by 0.6 to 1.0 dex. In the case of NGC 1818/D1 (the only spectroscopic main sequence star in our sample), this enrichment is coupled with a depletion of C and an enrichment of He, strongly suggesting that these abundances have already been altered through some kind of mixing with CNO-processed material.

Key words: stars: abundances – stars: atmospheres – stars: early-type – stars: evolution – galaxies: Magellanic Clouds

1. Introduction

The overall metal deficiency of the Magellanic Clouds (MCs) is a long-established fact, yet the homogeneity of this depletion within each cloud has been in dispute for many years: from early photometric (and some of the subsequent spectroscopic) studies the young populous clusters (YPCs) were thought to be significantly underabundant with respect to the field populations which surround them. To exemplify this, Table 1 lists the results of various works on NGC 330, the best-studied YPC in the SMC (a similar compilation could be presented for e.g. NGC 1818 in the LMC). Up to the early 1990 s, differences up to 0.5 dex were found (a development that culminated in a scenario by Richtler und Seggewiß (1988) which favoured the formation of clusters from metal-poor gas), since then a trend towards unanimity can be noticed. Retrospectively, a major part of the discrepancies can be attributed to the (initially unknown and) non-uniform reddening which enters whenever photometric quantities are used, even in "spectroscopic" studies which derive stellar parameters photometrically (e.g. Spite et al. 1986). The remaining discrepancies prompted us to re-evaluate the results of Reitermann (1990) and Jüttner et al. (1993) using *purely spectroscopic means* and more sophisticated input physics. Two stars were added to the sample, AV 218, an SMC field giant, and D1, a main sequence star and possible member of the LMC cluster NGC 1818.

Table 1. A selection of results on the iron deficiency of the SMC cluster NGC 330 and its surrounding field. J&T = Jasniewicz & Thévenin, G&R = Grebel & Richtler, R&N = Richtler & Nelles and $[\mathrm{X/H}] \equiv \log(n_{\rm X}/n_{\rm H})_\star - \log(n_{\rm X}/n_{\rm H})_\odot$ as usual.

author(s)	$[\mathrm{Fe/H}]_{330}$	$[\mathrm{Fe/H}]_{\rm field}$	method
R&N (1983)	-1.8	–	$uvby$ photom.
Spite et al. (1986)	-1.4	–	high res. spec.
G&R (1992)	-1.26	-0.74	uby
J&T (1994)	-0.55	-0.46	medium res.spec.
Grebel (1995)	-0.76	-0.87	UBVRI photom.
Hill (1999)	-0.82	-0.69	high res.spec.

In addition to the above it is worthwhile analysing MC B stars on and close to the main sequence (MS) since a) their unevolved state limits the risk of determining abundances which do not reflect those of the progenitor ISM and b) they can bridge the gap between the atomic abundances observable in H II regions (He – Ar) and those accessible in cool supergiants (Na – Eu). In particluar, the elements C, N and O can be observed well in spectra of B stars thereby potentially constraining scenarios of MS rotational mixing (cf. Fliegner et al. 1996). If such mixing is indeed common among early-type stars, observing it on the MS is crucial to be able to distinguish it from signatures of later evolutionary phases, notably the first dredge-up.

2. Preselection of candidates

Since B stars are frequently fast rotators and/or show emission in their Balmer lines (Be stars, cf. Jaschek et al. 1981), a great effort

Send offprint requests to: A.J. Korn (ajkorn@usm.uni-muenchen.de)

⋆ Based on observations carried out at the European Southern Observatory, La Silla, Chile.

Table 2. Some of the stars that were observed at medium resolution and rejected due to the reason given in Column 4. BRU = Brunet et al. (1975), AV = Azzopardi & Vigneau (1975), nomenclature for the NGC objects from Robertson (1974).

object	MC	m_V [mag]	$v \sin i$ [km s^{-1}]
BRU 52	LMC	13.61	>100
BRU 56	LMC	13.87	>75
BRU 147	LMC	13.46	>100
BRU 182	LMC	13.74	>75
BRU 214	LMC	13.20	>75
BRU 251	LMC	13.83	>100
BRU 259	LMC	13.90	>100
NGC 1818/D14	LMC	13.37	Be
NGC 2004/B16	LMC	14.08	Be
NGC 2004/C17	LMC	14.68	Be
NGC 2100/C30	LMC	14.07	see text
NGC 2100/D31	LMC	14.77	see text
AV 163	SMC	14.18	>100
AV 178	SMC	14.38	>100
AV 196	SMC	13.93	>100
NGC 330/B21	SMC	14.29	Be
NGC 330/B22	SMC	14.23	Be, see text
NGC 330/B32	SMC	14.92	Be, see text

was made to select the small number of stars which are suitable for an abundance fine analysis: non-Be and with projected rotational velocities $v \sin i$ below 75 km s^{-1}. Accordingly, B stars with photometric spectral types B0 to B3 *located on the upper main sequence in cluster CMDs* of Robertson (1974) and field stars with corresponding colours were checked for being sharp-lined in the blue (4100 – 4500 Å) and non-Be in Hα (5700 – 6600 Å). Observations were carried out using both the ESO 1.5m and ESO/MPI 2.2m telescope, mostly as part of the ESO key programme "Coordinated Investigations into Selected Regions of the Magellanic Clouds" (de Boer et al. 1989). In both cases the telescope was equipped with a Boller & Chivens spectrograph (Heydari-Malayeri et al. 1989) to yield dispersions between 30 and 116 Å/mm. In most cases the brightest stars fulfilling the above criteria were chosen to stay within the limits of reasonable exposure times for the follow-up high resolution observations with CASPEC. An upgrade of CASPEC between the 1991 and 1993 run allowed spectra of fainter stars (in particular NGC 1818/D1) to be obtained. The success rate of individual preselection runs between 1987 and 1993 varied from 5 to 30 %.

Table 2 lists a portion of the stars that were rejected due to the aforementioned reasons. It is important to note that due to the presence of diffuse (and patchy) H II emission prevailing the cluster fields it is not always easy to discern *intrinsic* non-Be stars unambiguously. In cases of doubt, the stars were rejected (but see Keller & Bessell 1998 who find NGC 330/B22 and B32 to be non-Be).

3. Observations

The spectra of the selected programme stars were taken using CASPEC on the 3.6m telescope of ESO, La Silla, Chile during sessions between 1986 and 1993. A detailed description of the 1987 CASPEC observations, the reduction procedure, the tracings of the spectra ($4000 < \lambda < 5000$ Å) for NGC 1818/D12, NGC 2004/B30 (both LMC) and NGC 330/B30 (SMC, nomenclature from Robertson 1974) and a list of identified lines is given in Jüttner et al. (1989). The data reduction was carried out using standard procedures supplied in MIDAS augmented by an optimal extraction algorithm for cosmic ray removal (cf. Horne 1986). Special care was taken to correct for the blaze function. The blaze correction was done in the two-dimensional pixel-order frame and interpolation was used for orders containing Balmer lines. This procedure yields continuum rectification results superior to the one-dimensional case. The individual exposures were finally added and averaged. Table 3 gives a brief observation log for all programme stars. As can be seen, an average signal-to-noise ratio (S/N) of 110 was achieved at R $\sim$ 20 000.

Table 3. Observation log for the programme stars. The line-free wavelength ranges 4202 – 4210, 4402 – 4409, 4493 – 4500 and 4680 – 4695 Å were used to estimate the S/N ratios (1σ).

object	MC	m_V [mag]	t_{exp} [h]	S/N	m/y
BRU 217	LMC	13.40	2.0 + 2.5	80	1/91
BRU 231	LMC	13.10	2.0	80	1/91
NGC 1818/D1	LMC	14.93	3.0 + 3.0	120	12/93
NGC 1818/D12	LMC	13.74	3 x 1.5	150	11/87
NGC 2004/B15	LMC	14.18	3.0 + 3.0	70	12/89
NGC 2004/B30	LMC	13.83	3 x 2.0	150	11/87
AV 175	SMC	13.65	2.0 + 2.5	100	12/89
AV 218	SMC	13.80	2.5 + 2.5	160	12/93
NGC 330/B30	SMC	14.19	2.0 + 2.0	90	11/87

4. Model atmosphere analysis

An indispensable prerequisite for the reliable determination of absolute abundances is the accurate measurement of profiles or equivalent widths. The main source of uncertainty entering here is the continuum definition. In principle, the continuum can be defined well with the help of line-free spectral regions in between the relatively few lines in B-star spectra. However, a certain amount of subjectivity remains, e.g. through ignorance about the absence/presence of weak lines, resulting in the over/underestimation of equivalent width. To circumvent this problem, we use an LTE utility (Gummersbach & Kaufer 1996) that takes all spectral lines of Kurucz & Bell (1995) into account. Specifically designed for main sequence stars from 10 000 to 35 000 K it is not only a valuable help for finding the continuum, it can also be used to identify unblended (strategic) lines as a function of temperature. The strategic silicon and oxygen lines (cf. 4.3) and those of all other elements considered here were selected using this tool (for computational details see URL of Gummersbach & Kaufer 1996).

The classical method of analysing B star spectra makes use of three criteria to determine the stellar parameters:

1) Balmer line(s) (profile or equivalent width) for $\log g$,

2) an ionization equilibrium (e.g. Si II/III, III/IV or He I/II) to determine $T_{\rm eff}$ and
3) weak and strong lines of O II to fix the microturbulence ξ by demanding that there must not be a trend of abundance with equivalent width (Gehren 1988, Kaufer et al. 1994, Kilian-Montenbruck et al. 1994).

In principle, all steps are inter-related and depend on metallicity which is a priori unknown. One way of tackling this problem is to *assume* a more or less appropriate metallicity, e.g. $[m/{\rm H}] = -0.5\,(-1.0)$ for the LMC (SMC) as done by Reitermann et al. (1990) and Jüttner et al. (1993). It would, however, be desirable to derive $T_{\rm eff}, \log g$ and ξ *simultaneously* and to treat the metallicity in a self-consistent manner. Such an approach was developed by Gummersbach et al. (1998) which we follow in this analysis. We refer the reader to their paper for more details and an extensive parameter study.

4.1. LTE model atmospheres

We use the ATLAS 9 model atmosphere code (Kurucz 1993a) in its UNIX version by Lemke (1995). It produces plane-parallel, homogeneous and static atmospheres in local thermodynamic equilibrium (LTE) which are practically fully line-blanketed taking into account the effects of 58 million lines on the atmospheric structure. The necessary information on atomic transitions is available in the form of opacity distribution functions (ODFs) as a function of metallicity ($[m/{\rm H}] = 0, -0.5, -1.0$) on CD-ROM (Kurucz 1993b c).

A number of parameters can be set to various values. After a thorough inspection of their respective influence on the atmospheric structure (see Gummersbach et al. 1998), we settled for the following values: 15 iterations (maximum value), 64 depth levels (maximum value), $-5 \le \log\tau \le +4$, frequency grid 'LITTLE' (1212 points) and $\xi_{\rm atmo} = 8\,{\rm km\,s^{-1}}$. The choice of the atmospheric microturbulence is uncritical and does not influence the microturbulence (denoted by ξ without a subscript) to be derived from the line analysis.

4.2. Non-LTE line formation

While the line blanketing originating from tens of millions of weak lines can justifiably be treated in LTE, non-LTE *line formation* is essential and a step towards a more realistic treatment of the conditions in early-type stellar atmospheres. We use the non-LTE line formation code DETAIL/SURFACE of Butler & Giddings (1985), specifically the DETAIL version of Butler (1996) and the SURFACE version of Becker (1997). The following model atoms were used:

H I + He I/II (Husfeld 1996)
C II (Eber & Butler 1988)
N II (Becker & Butler 1988c, 1989)
O II (Becker & Butler 1988a, b)
Mg II, Si II/III/IV (Becker & Butler 1990a b)
Al III (adapted from Dufton et al. 1986)
Fe III (Vrancken et al. 1999)

We explicitly include the microturbulence derived from silicon and oxygen lines in the statistical equilibrium calculation in DETAIL. Doing so an inconsistency described by McErlean et al. (1998) is avoided for stars whose microturbulence velocity is found to be in excess of individual ionic thermal velocities $v_{\rm th} = \sqrt{2kT/m_{\rm i}}$ ($m_{\rm i}$ being the atomic mass of the ion considered).

4.3. Model grids

Judging from the analysis of Jüttner et al. (1993) the stellar parameters of the programme stars were expected to lie between 18 000 and 24 000 K in $T_{\rm eff}$ and 2.5 and 3.5 in $\log g$. We therefore constructed model grids of the following dimensions:

$T_{\rm eff}$ = 15 000... 30 000 K, $\Delta\,T_{\rm eff}$ = 1000 K
$\log g$ = 2.2... 4.5, $\Delta \log g$ = 0.1 dex
$[m/{\rm H}] = 0, -0.5, -1.0$

The helium abundance is varied with $[m/{\rm H}]$ between ε(He) = 10.99 (the Solar value, cf. Grevesse et al. 1996) and ε(He) = 10.90 ($\sim$ primordial and H II$_{\rm SMC}$ value, cf. Olive & Steigman 1995 and Dufour 1984). The convergence is limited towards the Eddington limit resulting in a non-rectangular parameter space $\log T_{\rm eff} - \log g$ (cf. Fig. 2). All steps of the analysis (see Sects. 4.4 to 4.6) are calculated and presented in this $\log T_{\rm eff} - \log g$-diagram, sometimes referred to as "Kiel diagram" (Fuhrmann 1998).

An individual model grid is needed for every step of the analysis.

Balmer grid: At every grid point theoretical profiles of Hγ and Hδ are calculated *as a function of metallicity* $[m/{\rm H}]$. Since neither ξ nor $v \sin i$ has a noticeable effect on the profiles (if one disregards the central 3 Å), metallicity is the only dependence which needs to be considered. These profiles can thus be compared to observed profiles in a straightforward way (variance analysis, see Sect. 4.4).

Silicon grid: For a given set of stellar parameters $\{T_{\rm eff}, \log g\}$ the equivalent width of an atomic line depends on abundance, microturbulence and the metallicity of the underlying atmosphere. Lines which are far from their line-strength maximum are temperature sensitive and react to a change in metallicity: an increased metallicity results in more line blanketing in the depths of line formation which in turn mimics a hotter atmosphere. At every grid point theoretical equivalent widths are calculated using $\xi = 0, 2, 4, ..., 14\,{\rm km\,s^{-1}}$ and ε(Si) = 7.6, 7.1, 6.6[1] coupled with the respective metallicity $[m/{\rm H}]$ appropriate for the abundance of silicon in use, e.g. ε(Si) = 7.1 corresponds to $[{\rm Si/H}] = -0.5$ therefore demanding the use of a metallicity of $[m/{\rm H}] = -0.5$. This way, the required concordance between line abundance and overall metallicity is secured in a simple way. For any given ξ the three resulting equivalent widths ($[m/{\rm H}] = [{\rm Si/H}] = 0, -0.5, -1$) are interpolated via a logarith-

[1] $\varepsilon({\rm X}) := \log(n_{\rm X}/n_{\rm H}) + 12$.

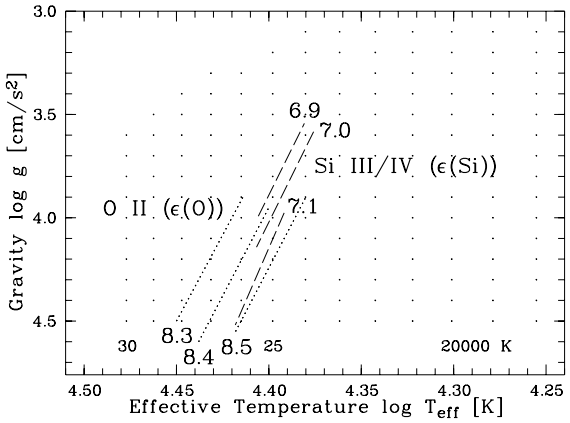

Fig. 1. Fits minimizing the difference between theory and observation for the silicon and oxygen analysis, here as a function of abundance. Abundances of silicon (6.9–7.1) on top, those of oxygen (8.3–8.5) at the bottom.

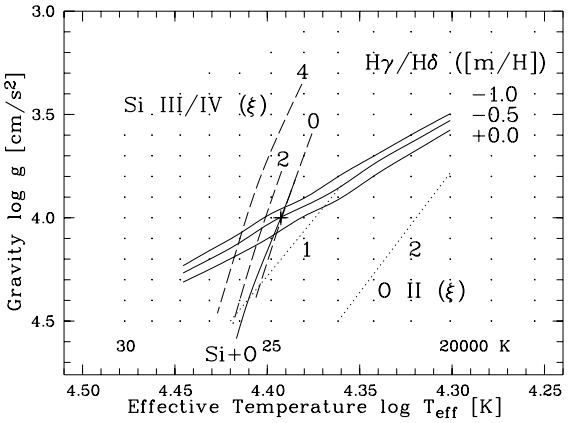

Fig. 2. All three steps of the analysis: silicon and oxygen analysis as a function of microturbulence (in units of km s^{-1}), Balmer analysis as a function of $[m/\mathrm{H}]$. Note that in comparing with Fig. 1 the abundances at the deduced stellar parameters (+) are ε(Si) = 7.10 and ε(O) = 8.46 demanding $[m/\mathrm{H}]_{\mathrm{Balmer}} = -0.44$.

mic cubic spline to obtain equivalent widths for ε(Si) = 6.6 to 7.6 in steps of 0.1 dex. Grids were calculated for the following lines:

Si II 4128, 4131, 5056,
Si III 4553[2], 4568, 4575,
Si IV 4116.

Oxygen grid: Based on the same grid of model atmosphere calculations and the same values of ξ, a grid of equivalent widths as a function of abundance (ε(O) = 8.9, 8.4, 7.9) was calculated for the following unblended oxygen lines:

O II 4079, 4367, 4415, 4452, 4591, 4596,
4649, 4662, 4676, 4696, 4701, 4703, 4941, 4943

Again, when using the Solar value for oxygen (ε(O) = 8.9) a Solar atmospheric metallicity is assumed, correspondingly ε(O) = 7.9 requires the use of a metallicity of 1/10 Solar. For a given ξ interpolation is performed between the three resulting equivalent widths at every grid point to obtain a step size of 0.1 dex in abundance.

4.4. The Balmer analysis

For a meaningful comparison between theoretical and observed profiles a thorough wavelength calibration and flux normalization is needed. This is achieved by applying our LTE utility and the line-free spectral regions 4298 – 4302 Å/4397 – 4403 Å for Hγ and 4049 – 4052 Å/4134 – 4137 Å for Hδ.

The next step is to free the Balmer line wings from metal lines. Most of them are easily eliminated by mirroring the wings on top of each other and either taking the higher flux value (whenever the discrepancy exceeds that induced by the local noise) or the mean (when the difference is not significant in terms of the S/N). This procedure is based on the assumptions that the Balmer profiles are symmetric and that there are no emissions present. The thus restored profile $f_{\lambda,\mathrm{obs}}$ is smoothed and reduced to 18.5 Å of its red wing which can then be compared to theoretical profiles $f_{\lambda,\mathrm{th}}$. Minimizing the difference

$$\Delta_{\mathrm{H}} = \sum_{\lambda=4341.96}^{4360.46} (f_{\lambda,\mathrm{th}} - f_{\lambda,\mathrm{obs}})^2, \delta\lambda = 0.01\text{Å}$$

for a given T_{eff} and $[m/\mathrm{H}]$ yields the $\log g$ at which the observed profile is fitted best. The final result of this step are fits as a function of $[m/\mathrm{H}]$. As can be seen from Fig. 2, metallicity does have an effect on these curves amounting to < -0.15 dex in $\log g$ when going from Solar to 1/10 Solar metallicity.

4.5. The silicon analysis

Keeping in mind that a self-consistent treatment of the metallicity was achieved by coupling the metallicity $[m/\mathrm{H}]$ to ε(Si) (refer back to 4.3) the remaining dependencies are silicon abundance and microturbulence (since we measure equivalent widths $v \sin i$ does not enter). In any given calculation one of these two parameters can be kept fixed while the other one is varied. The results are fits both as a function of ε(Si) and of ξ which simultaneously reproduce the measured equivalent widths of two adjacent ionization stages of silicon. Fig. 1 shows the fits as a function of ε(Si), Fig. 2 those for ξ as the varying parameter. Comparing the two sets of fits one notices that they are inclined with respect to one another, a natural consequence of the fact that their respective dependencies are reversed.

4.6. The oxygen analysis

Instead of demanding that the slope of a linear regression line vanishes in the $\mathrm{W}_\lambda - \varepsilon$(O) plane (the classical procedure) we minimize

$$\Delta_{\mathrm{O}} = \sum_{\mathrm{O\,II\ lines}} (\mathrm{W}_{\lambda,\mathrm{theo}} - \mathrm{W}_{\lambda,\mathrm{obs}})^2$$

at every grid point for a given ε(O) and varying microturbulence[3]. Done for all applicable oxygen abundances, the minima found in this procedure define a new function whose minimum can be sought via a cubic spline. This minimum constitutes the pair $\{\varepsilon(\mathrm{O}), \xi\}$ which describes the observed equivalent widths best *at the chosen grid point*. This way one can, at least in principle, fill the whole parameter space with information on $\{\varepsilon(\mathrm{O}), \xi\}$ as presented in Figs. 1 and 2.

Note that for the latter two parts of the analysis the metallicity dependence is not as visible as in the case of the Balmer analysis, but rather it is implicit in the model grid calculation (cf. 4.8).

4.7. Putting the three steps together

We are now in a situation to put the three steps of the analysis (which have so far been fully independent of one another) together: this is done in Fig. 2 for NGC 1818/D1.

In a first step the silicon and oxygen analyses are combined by demanding that both species are subject to the same microturbulence. This condition precludes us from finding larger ξ from oxygen lines ($\xi(\mathrm{O}) - \xi(\mathrm{Si}) \sim 5\,\mathrm{km\,s^{-1}}$) as in supergiants studied by McErlean et al. (1999). In their analysis the microturbulence from oxygen lines is not included in the derivation of the stellar parameters, but subsequently determined. On the solid curve labelled "Si+O" in Fig. 2 the microturbulence thus varies unanimously for silicon and oxygen.

In a second step this curve is matched up with the Balmer analysis fits. For this purpose the silicon and oxygen fits as a function of abundance are needed which have been omitted for clarity of presentation, but which are presented in Fig. 1. The final residual uncertainty about the stellar parameters is removed by demanding that $[m/\mathrm{H}]_{\,\mathrm{Balmer}} = \frac{1}{2}([\mathrm{Si/H}] + [\mathrm{O/H}])$, thus making use of the "representativeness" of the silicon and oxygen abundance for the metallicity once more. Since the "Si+O" curve is hardly a function of T_{eff} this is merely a final adjustment of $\pm\,0.1$ dex in $\log g$. At this point, the five parameters $T_{\mathrm{eff}}, \log g$, ξ, ε(Si) and ε(O) have been determined *simultaneously*. The projected rotational velocity $v \sin i$ can now be fixed by calculating the stellar model appropriate for the derived parameters (in terms of the metallicity this requires interpolation between adjacent ATLAS 9 models) and checking the profiles of the strategic silicon and oxygen lines. Now all parameters are available to calculate the profiles of the other ions (He I/II, C II, N II, Mg II, Al III and Fe III) as a function of abundance. Observed profiles of selected lines can then be compared directly to the synthetic ones as a function of abundance without the need of measuring equivalent widths.

4.8. Errors

One virtue of the analysis presented here is the fact that errors can be traced throughout the analysis. We have performed such error calculations two of which are presented below.

[3] These two procedures give entirely equivalent results, the latter is simply more efficient to carry out for a large number of grid points.

1. Error introduced by neglecting the appropriate metallicity
Here we consider the error in the silicon and oxygen analysis if one fails to bring the ion abundance into concordance with the overall metallicity. We start out with a fictitious star defined by its parameters $T_{\mathrm{eff}} = 25\,000$ K, $\log g = 4.0$, $\xi = 5\,\mathrm{km\,s^{-1}}$ and $[m/\mathrm{H}] = 0.0$ dex. As far as the ionic abundances of silicon and oxygen are concerned, we take this star to be metal-poor with $\varepsilon(\mathrm{Si}) := 6.76$ and $\varepsilon(\mathrm{O}) := 8.07$. According to ATLAS 9 and DETAIL/SURFACE these parameters result in the following line strengths:

W_λ(Si III 4568) = 109 mÅ
W_λ(Si IV 4116) = 31 mÅ
W_λ(O II 4415) = 102 mÅ.

We repeat this calculation, this time using $[m/\mathrm{H}] = -0.8$ dex, the lowest metallicity encountered in this project (cf. Table 4) and in harmony with the silicon and oxygen abundances used. The resulting equivalent widths are

W_λ(Si III 4568) = 107 mÅ
W_λ(Si IV 4116) = 19 mÅ
W_λ(O II 4415) = 87 mÅ.

Since the Si III line is close to its line strength maximum, the slight temperature change at line formation depth in the atmosphere does not significantly alter its equivalent width. Unlike Si III, both Si IV and O II lines are a few thousand degrees from their respective line strength maxima (28 000 K for O II and 31 000 K for Si IV at the given $\log g$) which leads to a stronger reaction to the change in atmospheric temperature structure. The resulting decrease in equivalent width is not dramatic taken as an isolated effect (it is in fact of the order of the uncertainty introduced by the noise), but taking into account that this effect results in a systematic offset of the stellar parameters, matters become more critical. The introduced deviations can also be expressed in terms of the stellar parameters by asking which parameters are needed to reproduce the original equivalent widths of silicon for $[m/\mathrm{H}] = -0.8$ dex. Keeping ξ fixed the stellar parameters are $T_{\mathrm{eff}} \sim 26\,000$ K and $\log g \sim 4.0$. As shown below $\Delta\, T_{\mathrm{eff}} = 1000$ K is of the order of the overall internal error and therefore a significant deviation from the *intrinsic* temperature of a metal-poor star.

2. The overall internal error of the analysis
The overall error is dominated by the error potentially made when determining the local continuum level. As an *upper limit* to errors of that sort in spectra with S/N ~ 100 we deliberately deviated from the optimal continuum level for NGC 1818/D1 by 1 % in such a way as to decrease the values of the stellar parameters. The three steps of the analysis still converge on their own. Bringing them together yields the following minimum stellar parameters:

$T_{\mathrm{eff}} = 23\,800$ K, $\log g = 3.8$, $\xi = 1\,\mathrm{km\,s^{-1}}$,
$\varepsilon(\mathrm{O}) = 8.25$, $\varepsilon(\mathrm{Si}) = 6.88$.

These have to be compared with the results for NGC 1818/D1 presented in Table 4. We therefore believe that the abundances of He I/II, N II, O II and Si II/III/IV deduced are accurate to within 0.2 dex. C II, Mg II, Al III and Fe III are only represented

Table 4. Derived stellar parameters and abundances for the nine programme stars.

object	$T_{\rm eff}$ [K]	$\log g$	ξ [km s^{-1}]	$v \sin i$ [km s^{-1}]	ε(He)	ε(C)	ε(N)	ε(O)	ε(Mg)	ε(Al)	ε(Si)	ε(Fe)	$[m/\mathrm{H}]$ "(Si+O)/2"
$\odot$					*10.99*	*8.55*	*7.97*	*8.87*	*7.58*	*6.49*	*7.56*	*7.50*	
BRU 217	18 100	2.66	11	35	10.80	–	7.60	8.42	6.90	5.80	7.12	6.95	−0.45
±	*700*	*0.15*	*1*	*10*	*0.2*	–	*0.2*	*0.2*	*0.3*	*0.3*	*0.2*	*0.3*	
BRU 231	17 600	2.46	14	45	10.90	(7.8)	7.90	8.40	7.00	5.80	7.05	7.04	−0.49
±	*700*	*0.15*	*1*	*10*	*0.2*	–	*0.2*	*0.2*	*0.3*	*0.3*	*0.2*	*0.3*	
NGC 1818/D1	24 700	4.00	0	30	11.11	7.83	7.59	8.46	7.35	6.03	7.10	7.34	−0.43
±	*1000*	*0.20*	*1*	*10*	*0.2*	*0.3*	*0.2*	*0.2*	*0.3*	*0.3*	*0.2*	*0.3*	
ε(X) (LTE)					11.09	7.91	7.72	8.68	7.47	6.03		7.37	
NGC 1818/D12	16 850	2.83	4	40	10.90	(8.1)	8.00	8.45	6.75	5.80	6.90	–	−0.54
±	*700*	*0.15*	*1*	*10*	*0.2*	–	*0.2*	*0.2*	*0.3*	*0.3*	*0.2*	–	
NGC 2004 /B15	19 900	3.11	6	25	10.85	7.90	–	8.35	6.78	5.90	6.74	7.05	−0.67
±	*1400*	*0.20*	*2*	*15*	*0.3*	*0.3*	–	*0.3*	*0.4*	*0.4*	*0.3*	*0.4*	
NGC 2004/B30	23 450	3.34	14	30	10.90	(7.6)	7.50	8.35	7.00	5.80	6.90	7.08	−0.59
±	*900*	*0.20*	*1*	*10*	*0.2*	–	*0.2*	*0.2*	*0.3*	*0.3*	*0.2*	*0.3*	
$\bar{\varepsilon}(\mathrm{X})_{\rm LMC}$					10.91	7.85	7.72	8.41	6.96	5.86	6.97	7.09	
±					*0.12*	*0.18*	*0.22*	*0.05*	*0.22*	*0.09*	*0.15*	*0.15*	
H II $_{\rm LMC}$					10.95	7.90	6.90	8.40	–	–	6.70	–	
AV 175	19 200	2.67	13	30	10.90	–	7.30	8.20	6.60	5.45	6.90	6.64	−0.67
±	*1400*	*0.20*	*2*	*15*	*0.3*	–	*0.3*	*0.3*	*0.4*	*0.4*	*0.3*	*0.4*	
AV 218	23 100	2.93	13	65	10.90	7.50	7.20	8.00	6.90	5.70	6.80	6.99	−0.82
±	*900*	*0.15*	*1*	*10*	*0.2*	*0.3*	*0.2*	*0.2*	*0.3*	*0.3*	*0.2*	*0.3*	
NGC 330/B30	16950	2.77	6	45	10.90	(7.3)	–	8.25	6.85	–	6.82	–	−0.68
±	*1400*	*0.20*	*2*	*15*	*0.3*	–	–	*0.3*	*0.4*	–	*0.3*	–	
$\bar{\varepsilon}(\mathrm{X})_{\rm SMC}$					10.90	7.40	7.25	8.15	6.78	5.58	6.84	6.82	
±					–	*0.14*	*0.07*	*0.13*	*0.16*	*0.18*	*0.05*	*0.25*	
H II $_{\rm SMC}$					10.91	7.40	6.50	8.00	–	–	6.30		

by one to four lines in the spectra, thus an error of 0.3 dex seems appropriate. The stellar parameters $T_{\rm eff}$ and $\log g$ are known to within 5 %.

For three stars (NGC 2004/B15, AV 175 and NGC 330/B30) the oxygen analysis did not converge uniquely due to either the weakness or the paucity of strategic lines available in the observed spectrum. Instead of disregarding these stars altogether, we derive stellar parameters mostly based on the Balmer and silicon analyses. The microturbulence is thus no longer concordantly derived between silicon and oxygen and formal errors a factor of 1.5 larger are assigned to these objects.

When comparing the model fits to the observed spectrum in Fig. 3 one notices the unsatisfactory reproduction of the Balmer line cores. This is generally found (cf. Gummersbach et al. 1998; Vrancken et al. 1997), but goes in the opposite direction in our giant stars (over-reproduction). This effect can be explained by the larger extension of giant star atmospheres and the gradual break-down of the plane-parallel approximation (wind emission). Since the $\log g$ information is contained in the Balmer *wings*, our analysis is not affected by this deficit.

We can now address the question of how well silicon and oxygen trace the overall atmospheric metallicity, in other words whether the representativeness of Si and O is a justifiable assumption: on average, $[m/\mathrm{H}]$ from Si and O complies with $[\mathrm{Fe/H}]$ on the 0.1 dex level. A slight shift was expected from the $[\alpha/\mathrm{Fe}]$ ratios peculiar to the MCs (see below).

5. Discussion

The stellar parameters of the programme stars (cf. Table 4) turn out somewhat lower than the LTE parameters derived by Jüttner et al. (1993), a direct result of the intrinsically greater non-LTE line strengths. The effective temperature of NGC 1818/D12 and NGC 330/B30 are now, for the first time, compatible with the reddening-free Q value of Reitermann et al. (1990) to within 500 K. A trend to smaller microturbulences is noticeable, again as expected from a transition from LTE to non-LTE. While NGC 1818/D1 is definitely a main sequence star, the evolutionary status of the other eight stars is uncertain: despite being MS stars photometrically they fall into a region of the HRD (the so-called Blue Hertzsprung Gap, cf. Fig. 4) which ought to be only scarcely populated since it is crossed very rapidly according to stellar evolutionary theory. The absence of this gap in the MCs has already been noticed by Fitzpatrick and Garmany (1990). Grebel (1995) discusses options for the nature of objects located in the gap. Contrary to what she concludes, the significant N enhancement found in these stars characterizes them as being *evolved* (not to be equated with having been RSGs, see

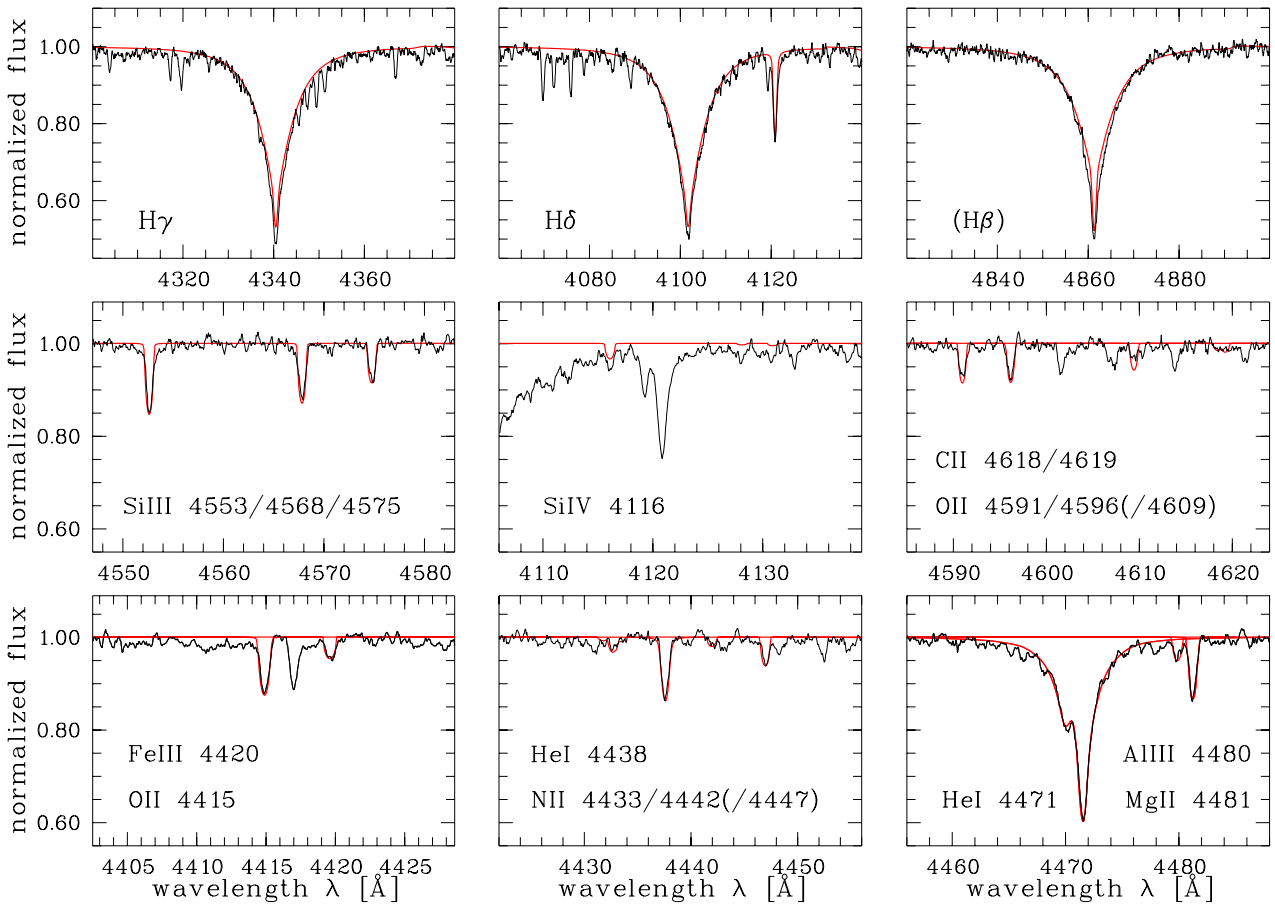

Fig. 3. Comparison between the observed spectrum of NGC 1818/D1 and the non-LTE model fits for various ions. Some strategic lines are labelled, others (those in parentheses) are indentified for illustration. Note that e.g. Si IV 4116 does not follow the pseudo continuum of Hδ, because every ion is treated individually in DETAIL/SURFACE.

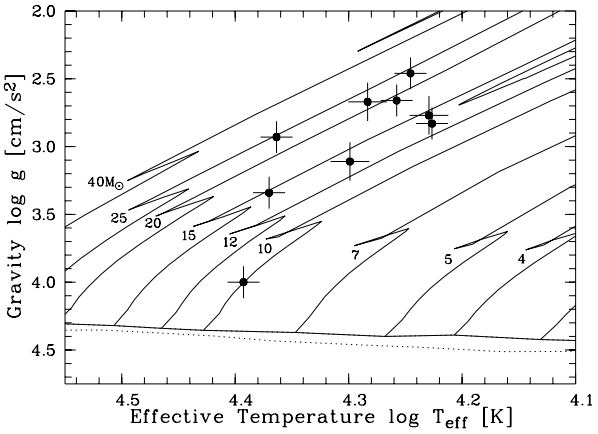

Fig. 4. Kiel diagram showing the loci of the programme stars with respect to evolutionary tracks according to Schaerer et al. (1993) for Z = 0.008. A zero-age main sequence (ZAMS) for Z = 0.004, more appropriate for the SMC stars, is indicated by the dotted line.

below). We believe that choosing the brightest objects in our preselection resulted in mainly finding this particular kind of stars.

Three of these stars (Bru 217 & 231, AV 175) are assigned to luminosity class Ib when the classification of Humphreys & McElroy (1984) is used. Interestingly, they have $v \sin i$ lower than any of the roughly 100 B supergiants earlier than B5 analysed by Howarth et al. (1997) who find a lower limit for $v \sin i$ of 50 km s^{-1}. They attribute this minimum to the presence of an additional, non-thermal line broadening mechanism and hypothesize on effects due to radiation-driven winds. One would then expect this effect to scale with metallicity. The fact that we do find B supergiants with $v \sin i$ as low as 30 km s^{-1} in the MC could be taken as an indication that the physical nature of this broadening is indeed related to wind phenomena. Further studies are needed here.

Before definite conclusions can be drawn with respect to potential abundance differences between cluster member and field stars, the question of cluster membership of each NGC star has to be settled. For NGC 330/B30 membership is most probable since its heliocentric radial velocity of 146 km s^{-1} compares favourably with that deduced for the cluster itself, $v_{\rm rad}^{330} = 147 \pm 1$ km s^{-1} according to Maurice et al. (1989). The same authors deduce $v_{\rm rad} = 114 \pm 4$ km s^{-1} for the surrounding field. The difference in radial velocity is therefore large enough to discrimintate between cluster members and field stars.

For the LMC clusters the situation is more difficult: differences between cluster radial velocities and those of the surrounding fields are very small, if not vanishing (Freeman et al. 1983). Considering the youth of these objects (cf. 5.2) this comes as no surprise. All we can say from radial velocities is that membership is unlikely for NGC 2004/B15 as its $v_{\rm rad}$ is 40 km s^{-1} higher than the cluster mean (349 ± 10 km s^{-1} vs. 309 ± 11 km s^{-1}, Freeman et al. 1983).

We can also resort to purely geometrical considerations: for each cluster a (projected) radius can be defined beyond which the density has reached that of the surrounding field. For NGC 1818 this *field density radius* is $r_{\rm fd}$ = 140″, for NGC 2004 $r_{\rm fd}$ = 130″ (Keller, private communication). NGC 1818/D1 practically lies on $r_{\rm fd}$, whereas NGC 1818/D12 and NGC 2004/B30 fall well within these radii (at 0.5 respectively $0.3\,r_{\rm fd}$)[4]. Judging from this perspective, especially the cluster membership of NGC 1818/D1 is in doubt.

5.1. MC abundances

Table 4 lists all the derived abundances, their mean values $\bar{\varepsilon}(\mathrm{X})$ and the pristine H II values to which the prior ought to be compared (He from Russell & Dopita 1992, CNO and Si as reviewed by Garnett 1998). The best-observed element, oxygen, shows the highest internal consistency. Its averaged SMC values compares very favourably with the O abundances from A-type supergiants derived by Venn (1999). The nearly vanishing discrepancy between the B-star and H II oxygen speaks in favour of merely small external offsets which absolute abundances could be prone to. Inseparably, it leaves little room for large fractions of oxygen tied up in interstellar dust (such as the 45 % claimed by Meyer et al. (1998) for the Solar neighbourhood).

One safe conclusion can be drawn from the mean values and their scatter:

Within the given (*realistic*) accuracy no abundance differences are detected between cluster members and field stars in both Clouds.

In all but three cases the 1σ scatter is below 0.20 dex, fully compatible within the intrinsic uncertainty; it is slightly larger for nitrogen and magnesium in the LMC and iron in the SMC.

Magnesium: The scatter is mostly caused by $\varepsilon(\mathrm{Mg})_{1818/\mathrm{D1}}$ which is 0.6 dex higher than that of D12 displaying the lowest Mg abundance. Though these abundances are marginally compatible within the errors (the abundance is based on the well-observed Mg II 4481 doublet), we believe this discrepancy to be significant. Since there is no H II magnesium abundance to compare with, we have to check other sources to learn something about its pristine value: From medium-resolution spectra of 5 NGC 1818 supergiants Jasniewicz & Thévenin (1994) deduce [Fe/H] $\sim$ [Mg/H] ~ -0.4. Using CASPEC Richtler et al. (1989) find [Fe/H] ~ -0.91 for one supergiant in NGC 1818. It is therefore rather impossible to draw definite conclusions about the iron or magnesium deficiency of NGC 1818 from the spectroscopic literature. For two MS B stars in the LMC field Rolleston et al. (1996) deduce ε(Mg) = 7.0 respectively 7.4 in LTE, on average somewhat higher than our mean value and thus more compatible with the abundance found in D1. All in all these findings argue against a common origin of these two stars. Unless the abundances in D1 have been altered by e.g. mass transfer from an undetected companion, D1 is more likely to be a field star (for a more thorough discussion of D1 see the Sect. 5.2).

Another feature needs to be discussed: there are significant offsets between the mean values for nitrogen and their H II counterparts in both Clouds and between $\bar{\varepsilon}$(Si) and ε(Si) from H II in the SMC.

Nitrogen: An offset of 0.82 dex (LMC) and 0.75 dex (SMC) is hard to reconcile with the given H II value, even if dust depletion factors are considered (which are thought to be small anyway, Mathis 1996). Whereas it is not at all inconceivable to encounter completely different abundance ratios in different surroundings like the MCs, we are surprised to find that apart from the two most evolved LMC objects (BRU 231 and NGC 1818/D12) the $[\mathrm{N/O}]$ ratios are indistinguishable from those of Orion and the Sun: 0.05 ± 0.04. This result is in harsh contrast to the H II value of -0.6 in both clouds (Garnett 1998). If we do take the H II nitrogen abundance as the pristine value (see Dennefeld (1989) for a cautionary note), then the abundances found have to be called 'enriched' and are a clear indication that the atmospheres of *all* our programme stars (even of D1, see below) have been subject to evolutionary effects. Some stars could have already been on the red side of the HRD having experienced the FDU (which now places them on very extended blue loops, cf. Fig. 4), for others, notably D1 on the MS, this scenario seems highly unlikely. Rotational mixing will be discussed as one answer in the next section. If indeed more than one process is at work, a larger scatter in nitrogen abundances (cf. N in supergiants by Venn 1999) is to be expected: e.g. Lennon et al. (1996) find a even higher enrichment of 1.2 dex relative to H II for two MS B stars in NGC 330.

Silicon: By comparing H II log Si/O values with those derived from Galactic stellar samples, Garnett et al. (1995) derive dust corrections of 0.6 to 1.0 dex for silicon, e.g. up to 0.8 dex need to be invisible in Orion's H II to be compatible with the B-star silicon abundance of Gummersbach et al. (1998). These depletions could explain the offset of 0.54 dex found between the mean of the SMC programme stars and the H II value. For two SMC MS B stars Lennon et al. (1996) find a similar offset of $\bar{\varepsilon}$(Si) = 0.55 dex, a third star in NGC 330 shows silicon compatible with H II. Puzzling, however, is the fact that the difference between these two entities in the LMC is merely 0.27 dex requiring smaller dust corrections. A MS O star ($T_{\rm eff}$ = 32 000 K) in the LMC analysed by Rolleston et al. (1996) appears to be Solar in silicon. This would require a dust depletion approaching

[4] Note, however, that NGC 2004/B15, a radial velocity non-member, lies at $0.25\,r_{\rm fd}^{2004}$! Is it a "runaway" star whose space motion was changed when a hypothetical former companion exploded as a supernova?

1.0 dex. But this high abundance could also be due to the inappropriateness LTE for O stars (cf. Kudritzki & Hummer 1990). In this it might be illustrative to examine how large the non-LTE effects are. They are given in Table 4 for all abundances of NGC 1818/D1 except for silicon, because, as one would expect when calculating LTE abundances at non-LTE stellar parameters, the ionization equilibrium is no longer balanced. Si III would give 7.6, Si IV 7.3.

Helium: The derived helium abundances are completely compatible with their H II counterparts. Only in the case of NGC 1818/D1 an abundance significantly different from the H II value is found. The remarkable fit for He I 4471 (Fig. 3) and the fact that He I 4121 would even require an abundance of 11.2 illustrate and substantiate this claim. The modelling of He II 4686 (only observed in NGC 1818/D1) is also compatible with a significant helium enhancement and lends extra weight to the correctness of the temperature determination method. This He signature will be discussed further in the context of Sect. 5.2.

Carbon: The most prominent C II feature is the C II 4267 doublet which is known to be subject to strong non-LTE effects (Eber & Butler 1988). Despite working with non-LTE line formation in this analysis, the abundances solely based on this line (those in parentheses in Table 4) do not appear completely trustworthy to us, since e.g. this feature could not be modelled for NGC 1818/D1 whatsoever. A more comprehensive C II model atom presented by Sigut (1996) might be able to explain our modelling difficulties in NGC 1818/D1, as the difference in predicted equivalent width between the Eber & Butler (1988) and Sigut (1996) model vanishes below $T_{\rm eff} \sim 21\,000$ K, but rises to a maximum of 20 % near $T_{\rm eff} \sim 26\,000$ K (cf. Sigut 1996, his Fig. 1). Future work will take these modifications into consideration.

For three stars additional features were available for deriving ε(C), at least one of C II 4075, 4375, 4377, 4411, 4412, 4619. All of these are only visible and unblended down to about 20 000 K. Irrespective of whether we disregard or accept the carbon abundances based on C II 4267 the agreement with the H II data is excellent. Note, though, that according to Mathis (1996) up to 50 % of all interstellar carbon might be locked up in grains resulting in a present-day carbon abundance of 8.2 (LMC) respectively 7.7 (SMC). It is plausible to assume *some* depletion onto grains. We therefore adopt depletion factors such that the actual interstellar carbon abundances are taken to be 8.1 (LMC) and 7.6 (SMC).

Iron: A number of Fe III features are accessible in NGC 1818/D1 (Fe III 4081, 4137, 4139, 4165, 4420), but they soon vanish as the temperature decreases without being replaced by measurable Fe II lines. No iron abundance could therefore be determined for the two coolest stars, NGC 1818/D12 and NGC 330/B30. Average iron deficiencies of 0.4 (0.7) dex are derived for the LMC (SMC), canonical values when compared to the ample MC supergiant literature (e.g. Luck et al. 1998). NGC 1818/D1 seems slighty iron rich.

α-elements: Since we were not able to derive an iron abundance for NGC 330/B30, we cannot contribute to the ongoing discussion of the apparent stronger metal deficiency of NGC 330 with respect to the surrounding field, at least not in terms of $[\mathrm{Fe/H}]$. All we can say is that in terms of the α-elements O, Mg and Si the differences between the cluster and the field are vanishing: given equal weight[5] they agree to within 0.04 dex (1σ).

Generally speaking, $[\alpha/\mathrm{Fe}]$ in the MCs seems to behave differently from the Solar neighbourhood when comparing like with like in terms of metallicity (as noted numerous times in the literature): $[\alpha/\mathrm{Fe}] = +0.15$ (+0.25) at $[\mathrm{Fe/H}] = -0.4$ (-0.7) (F & G stars in the Solar neighbourhood, Edvardsson et al. 1993), but -0.12 in the MCs from this sample. Gonzalez & Wallerstein (1999) give a thorough discussion of this phenomenon. Ways of lowering $[\alpha/\mathrm{Fe}]$ are reviewed in Pagel & Tautvaišienė (1998).

5.2. A special case: NGC 1818/D1

We mentioned the possibility that some of our programme stars have already experienced the first dredge-up (FDU). The FDU brings to the surface the products of the CNO cycle, mainly helium and as a by-product nitrogen from the bottleneck reaction $^{13}\mathrm{C}(p,\gamma)^{14}\mathrm{N}$. Qualitatively, the expected signature is an increase in nitrogen (and to a lesser degree in helium) coupled with a corresponding depletion of carbon (and oxygen). Quantitatively, Schaerer et al. (1993) predict the following photospheric changes when a 10 $\mathrm{M}_\odot$ star with Z = 0.008 ($[m/\mathrm{H}] \sim -0.3$) undergoes FDU: ε(He) +0.05, ε(C) -0.18, ε(N) +0.50 and ε(O) -0.05. Paradoxically, it is the one MS star in our sample that shows such a signature, the only star whose evolutionary stage is known with certainty. Note that carbon is slightly down with respect to the assumed interstellar value, but still fully compatible with it in the given error limits. It will be a challenge for future work to lower the residual uncertainties to a point where such a small difference becomes significant. For the time being, it is tempting to think of this signature as an indication that there are processes which alter photospheric abundances of some B stars in a fashion similar to that of the FDU *already on the MS*. Analysing Galactic B stars Gies & Lambert (1992) draw a similar conclusion from the distributions of C, N and O in their sample.

Unfortunately, we cannot single out a process exclusively responsible for this phenomenon. Although we did not find evidence for radial velocity variations throughout our preselection and observing runs, binarity cannot be completely ruled out. It is therefore conceivable that D1 received processed material via mass transfer from an unseen companion. The significant Mg and slight Fe enhancement speak in favour of binary interaction (note, though, that oxygen and silicon behave rather normal).

If no external process were at work, mixing from the interior would have to explain this early abundance alteration. Such

[5] $[\alpha/\mathrm{H}] = \frac{1}{3}([\mathrm{O/H}] + [\mathrm{Mg/H}] + [\mathrm{Si/H}])$

mixing is usually attributed to effects of rotation currently unaccounted for in standard evolutionary theory (Zahn 1992; Maeder 1987; Langer 1992). In this scenario D1 would be a moderately or rapidly rotating star seen pole-on (the other programme stars would then be a mixture of pre- and post-RSG/intrinsically slow-rotating, pole-on and spun-down giants with nitrogen enhancement due to rotational mixing or FDU or both). If our sample stars have not experienced MS mixing, then a slow and continuous evolution to the red (cf. Schaller et al. 1992) can be ruled out in view of their HRD position coupled with the N enhancement found.

Note that rotation does not only alter photospheric abundances, it can also greatly affect evolutionary tracks and isochrones (cf. Fliegner et al. 1996). This is the reason why we did not derive ages for the giant stars in our sample. It is important to note, though, that the filling of the Hertzsprung gap (cf. Fitzpatrick & Garmany 1990) by these stars could be explained by a population of stars rotating at different rates (Langer 1993).

For NGC 1818/D1 an age was derived: using the appropriate tracks in terms of metallicity, we derive a "non-rotating" single-star age of (20 ± 2) Myr, at the lower end of what is suggested from cluster photometry for NGC 1818 by Will et al. (1995) who find 20 – 40 Myr using different stellar evolution models. If D1 were a rapidly rotating star, then this value would constitute a lower limit to the "rotating" age of this star since the effects of rapid rotation will tend to increase its main sequence life time.

Knowing the distance moduli of the MCs and applying an appropriate E_{B-V} to each star, one can derive luminosities and according positions in an H-R diagramme. In this procedure NGC 1818/D1 is the only star whose luminosity and mass turns out *higher* than expected (by 0.4 dex respectively 2 $M_\odot$). While this effect could simply be due to an erroneous determination of $\log g$, we believe it to be another indication for the rotational mixing scenario, as such stars do in fact evolve to higher luminosities (Fliegner et al. 1996).

6. Conclusions

We have reanalysed and extended the study of MC B stars done by Jüttner et al. (1993) employing non-LTE line formation and a consistent treatment of the atmospheric metallicity. We do not find significant abundance differences between likely cluster members and field stars within realistic error limits. The overall metallicity is deduced to be $[\mathrm{Fe/H}] \sim -0.4\,(-0.7)$ for the LMC (SMC), in line with a number of recent studies (Haser et al. 1998; Luck et al. 1998; Hill 1999; Venn 1999). The α-elements are found to be somewhat underabundant relative to iron, a finding shared by other absolute abundance analyses (Hill et al. 1997; Luck et al. 1998).

The MS star NGC 1818/D1 proves to be the most interesting star in our sample. On the one hand, the He and CNO signature – when compared to LMC H II – looks like that typical for the first dredge-up in the red-giant phase and is thus compatible with a MS mixing scenario (O and Si do not show an enhancement, as expected). On the other hand, Mg and Fe are enriched with respect to the mean value defined by the remaining LMC stars by 0.46 respectively 0.31 dex. Whereas binary mass transfer is capable of explaining the latter, rotational mixing is not. In that sense, the situation remains inconclusive.

Further studies of MC main sequence B stars are desperately needed to (among other things) obtain *a)* more information on the present-day MC abundances to set limits on the unknown dust depletions that hamper the interpretation of H II data and *b)* to verify or refute the importance of rotation and MS mixing in early-type stellar evolution (at least on a statistical basis). With the advent of 8m-class telescopes and highly efficient spectrographs B stars in MC clusters are ideal objects to tackle these kinds of problems.

Acknowledgements. This work was in part supported by the *Sonderforschungsbereich* SFB 328 "Entwicklung von Galaxien".

References

Azzopardi M., Vigneau J., Macquet M., 1975, A&AS 22, 285
Brunet J.P., Imbert M., Martin N., et al., 1975, A&AS 21, 109
Becker S.R., 1997, priv. comm.
Becker S.R., Butler K., 1988a, A&A 201, 232
Becker S.R., Butler K., 1988b, A&AS 74, 211
Becker S.R., Butler K., 1988c, A&AS 76, 331
Becker S.R., Butler K., 1989, A&A 209, 244
Becker S.R., Butler K., 1990a, A&AS 84, 95
Becker S.R., Butler K., 1990b, A&A 235, 326
Butler K., 1996, priv. comm.
Butler K., Giddings J.R., 1985, CCP7 Newsletter 9, 7
de Boer K.S., Azzopardi M., Baschek B., et al., 1989, ESO Messenger 57, 27
Dennefeld M., 1989, In: de Boer K.S., Spite F., Stasinska G. (eds.) Recent Developments of Magellanic Cloud Research. Observatoire de Paris
Dufour R.J., 1984, In: van den Bergh S., de Boer K.S. (eds.) IAU Symp. 108: Structure and Evolution of the Magellanic Clouds. Reidel, Dordrecht, p. 353
Dufton P.L., Brown P.J.F., Lennon D.J., Lynas-Gray A.E., 1986, MNRAS 222, 713
Eber F., Butler K., 1988, A&A 202, 153
Edvardsson B., Anderson J., Gustafsson B., et al., 1993, A&A 275, 101
Fitzpatrick E.L., Garmany C.D., 1990, ApJ 363, 119
Fliegner J., Langer N., Venn K.A., 1996, A&A 308, L13
Freeman K.C., Illingworth G., Oemler Jr. A., 1983, ApJ 272, 488
Fuhrmann K., 1998, A&A 338, 161
Garnett D.R., 1998, In: Chu Y.H., Szuntzeff N., Hesser J., Bohlender D. (eds.) New Views of the Magellanic Clouds. ASP, San Fransicsco, in preparation
Garnett D.R., Dufour R.J., Peimbert M., et al., 1995, ApJ 449, L77
Gehren T., 1988, Rev. Mod. Astron. 1, 52
Gies D.R., Lambert D.L., 1992, ApJ 387, 673
Gonzalez G., Wallerstein G., 1999, AJ 117, 2286
Grebel E.K., 1995, Ph.D. Thesis, Bonn
Grebel E.K., Richtler T., 1992, A&A 253, 359
Grevesse N., Noels A., Sauval A.J., 1996, In: Holt S.S., Sonneborn G. (eds.) Cosmic Abundances. ASP, San Fransisco, 117
Gummersbach C.A., Kaufer A., 1996, http://www.lsw.uni-heidelberg.de/cgi-bin/cgiwrap/cgummers/websynspec.cgi

Gummersbach C.A., Kaufer A., Schäfer D., Szeifert T., Wolf B., 1998, A&A 338, 881
Haser S.M., Pauldrach A.W.A., Lennon D.J., et al., 1998, A&A 330, 285
Heydari-Malayeri M., Jarvis B., Gilliotte A., 1989, The Boller & Chivens Spectrographs. ESO Opertaing Manual No. 9
Hill V., 1999, A&A 345, 430
Hill V., Barbuy B., Spite M., 1997, A&A 323, 461
Horne K.O., 1986, PASP 98, 609
Howarth I.D., Siebert K.W., Hussain G.A.J., Prinja R.K., 1997, MNRAS 284,265
Humphreys R.M., McElroy D.B., 1984, ApJ 284, 565
Husfeld D., 1996, priv. comm,
Jaschek M., Skettebak A., Jaschek C., 1981, Be star newsletter 4, 9
Jasniewicz J., Thévenin F., 1994, A&A 282, 717
Jüttner A., Reitermann A., Stahl O., Wolf B., 1989, A&AS 81, 93
Jüttner A., Stahl O., Wolf B., Baschek B., 1993, In: Baschek B., Klare G., Lequeux J. (eds.) New Aspects of Magellanic Cloud Research. Springer, Berlin, p. 337
Kaufer A., Szeifert T., Krenzin R., Baschek B., Wolf B., 1994, A&A 289, 740
Keller S.C., Bessell M.S., 1998, A&A 340, 397
Kilian-Montenbruck J., Gehren T., Nissen P.E., 1994, A&A 291, 757
Kudritzki R.P., Hummer D.G., 1990, ARA&A 28, 303
Kurucz R.L., 1993a, Kurucz CD-ROM No. 13: Atlas9 Stellar Atmosphere Program and 2 km s^{-1} Grid. Smithonian Astrophysical Observatory, Cambridge
Kurucz R.L., 1993b, Kurucz CD-ROM No. 2: Opacities for Stellar Atmospheres: $[+0.0]$,$[+0.5]$,$[+1.0]$. Smithonian Astrophysical Observatory, Cambridge
Kurucz R.L., 1993c, Kurucz CD-ROM No. 13: Opacities for Stellar Atmospheres: $[-0.5]$,$[-1.0]$,$[-1.5]$. Smithonian Astrophysical Observatory, Cambridge
Kurucz R.L., Bell B., 1995, Kurucz CD-ROM No. 23: Atomic Line List. Smithonian Astrophysical Observatory, Cambridge
Langer N., 1992, A&A 265, L17
Langer N., 1993, In: Weiss W.W., Baglin A. (eds.) Inside the Stars. ASP, San Fransisco, 426
Lemke M., 1995, ftp://ccp7.arm.ac.uk/ccp7/Soft/atlas.unix.tar.Z
Lennon D.J., Dufton P.L., Mazzali P.A., Pasian F., Marconi G., 1996, A&A 314, 243
Luck R.E., Moffett T.J., Barnes III T.G., Gieren W.P., 1998, AJ 115, 605
Maeder A., 1987, A&A 178, 159
Mathis J.S., 1996, ApJ 472, 643
Maurice E., Bouchet P., Martin N., 1989, A&AS 78, 445
McErlean N.D., Lennon D.J., Dufton P.L., 1998, A&A 329, 613
McErlean N.D., Lennon D.J., Dufton P.L. 1999, A&A 349, 553
Meyer D.M., Jura M., Cardelli J.A., 1998, ApJ 493, 222
Olive K.A., Steigman G., 1995, ApJS 97, 49
Pagel B.E.J., Tautvaišienė G., 1998, MNRAS 299, 535
Reitermann A., Baschek B., Stahl O., Wolf B., 1990, A&A 234, 109
Richtler T., Nelles B., 1983, A&A 119,75
Richtler T., Seggewiß W., 1988, In: Grindlay J.E., Davis Philip A.G. (eds.) Globular Cluster Systems in Galaxies. IAU Symp. 126, Kluwer, Dordrecht, p. 553
Richtler T., Spite M., Spite F., 1989, A&A 225, 351
Robertson J.W., 1974, A&AS 15, 261
Rolleston W.R.J., Brown P.J.F., Dufton P.L., Howarth I.D., 1996, A&A 315, 95
Russell S.C., Dopita M.A., 1992, ApJ 384, 508
Schaller G., Schaerer D., Meynet G., Maeder A., 1992, A&AS 96, 269
Schaerer D., Meynet G., Maeder A., Schaller G., 1993, A&AS 98, 523
Sigut T.A.A., 1996, ApJ 473, 452
Spite M., Caryel R., François P., Richtler T., Spite F., 1986, A&A 168, 197
Venn K.A., 1999, ApJ 518, 405
Vrancken M., Hensberge H., David M., Verschueren W., 1997, A&A 320, 878
Vrancken M., Butler K., Becker S.R., 1999, in preparation
Will J.-M., Bomans D.J., de Boer K.S., 1995, A&A 295, 54
Zahn J.P., 1992, A&A 265, 115